Observation of the Effect of Wetting Efficiency on a Flow of Liquids Impinging on Solid Substrates by Fluorescence Depolarization

Cristina M. Quintella*,† Cristiane C. Gonçalves,† Martha T. P. O. Castro,† Iuri M. Pepe,‡ Ana P. S. Musse,† and Ângelo M. V. Lima†

Instituto de Química and Instituto de Física, Universidade Federal da Bahia, Brazil

Received: November 12, 2002; In Final Form: May 22, 2003

Steady-state fluorescence depolarization has proven, in the past few years, to be a method sensitive to adhesion of thin liquid films flowing without boundaries on solid substrates of different chemical constitutions. This work extends our prior preliminary assessment of the efficiency of the method and the influence of experimental variables. Ten thin films of ethylene glycol (MEG) were mapped over 102 mm^2 by polarized laser-induced fluorescence (PLF−FI) while flowing on substrates. The interfacial tension, Γ_{SL}, was varied either by changing the chemical constitution of the substrate (borosilicate, tin dioxide, poly(vinyl alcohol) (PVA), and linear alkylbenzene sulfonate (LAS)) or by addition of tensoactives to MEG (sodium dodecyl sulfate (SDS) and poly(ethylene oxide) (PEO)). Contact angle measurements were employed to classify interfaces according to their static Γ_{SL}, that is, their wetting efficiencies. PLF−FI experimental variables, such as laser power, film thickness, and impinging velocity profile, did not alter the data within the range studied, except for flow rates over 220 cm s^{-1}. Average polarization (P_{av}) increased from 10.5% to 13.5% upon decreasing adhesion by varying the chemical constitution of the solid. When surfactants were dissolved in the liquid flow, polarization ranged from 5.4% to 3.8% while for surfactant as substrate it increased. Simple multivariate principal component analysis (PCA) was applied to downstream polarization averages (P_{down}) for each map. The two principal components accounted for 95.6% of the variance, ordering the maps according to decreasing adhesion and gathering them into three groups: dissolved surfactants, liquid films flowing at the highest flow rate, and solid surfaces of different chemical composition. Hierarchic cluster analysis (HCA) showed that, as adhesion decreased, similarity among the polarization maps increased.

Introduction

Recently, experimental improvements in techniques such as atomic force microscopy (AFM), scanning electronic microscopy, and low-angle X-ray reflection have made it possible to map surfaces with higher precision, including both structure and roughness. This allowed one to select interfaces with similar structure and roughness but different chemical constitutions. One can then relate chemical constitution to efficiency of interfacial processes and phenomena, ruled by interactions at the molecular level.

Contact angle (θ_c) measurements[1] are one of the experimental methods most used to study the solid−liquid interface. They permit the evaluation of the energy of interactions that take place both under static conditions and in systems where the liquid flows at quite low velocities. The relationship of θ_c to the static interfacial tension between solid and liquid (Γ_{SL}) provides information on wetting and adhesion and their dependence on type and direction of intermolecular forces at interfaces.

Interest in the influence of chemical composition on contact angle has increased since it has been shown that it is a predominant factor at many interfaces.[2−4] Recently, two different coexisting contact angles were observed for the same drop on a rubbed polymer and attributed to spatial asymmetry of interfacial chemical interactions.[5] Studies of drops moving at quite low velocity on solid surfaces showed that hysteresis (difference between the advancing and the receding θ_c) has a strong dependence on sorption[2] and arises primarily from molecular interactions between liquid and solid rather than surface roughness.[3]

It is known that an increase in the flow rate intensifies molecular effects compared to hydrodynamic effects,[1] increasing the contribution of chemical constitution and rendering chemical phenomena relevant. However, there is a lack of experimental techniques for observing, at the molecular level, liquids flowing at high flow rates on solid substrates.

Many important liquid−solid interfacial processes take place in liquid films flowing on solid substrates. These interactions depend on solid surface structure and roughness,[1] as well as on chemical constitution of the solid substrate[6] and the flowing liquid film.[7]

Steady-state fluorescence depolarization was recently applied[5−7] to study interfacial molecular interaction of fast flowing thin liquid films, flowing without boundaries, on solid substrates. It was found that flows on borosilicate could be differentiated from those on tin dioxide,[6] as well as from those of liquid films with two different dissolved tensoactive substances flowing on the same substrate.[7] These specific wettings were attributed to dynamic Γ_{SL} caused by the magnitude and direction of transient interactions between liquid flow and solid.

* To whom correspondence should be addressed. Address: Instituto de Química, Universidade Federal da Bahia, Campus de Ondina, CEP: 40.170-290, Brazil. Tel: 55-71-9987-0188. Fax: 55-71-235-5166. E-mail: cristina@ufba.br.

† Instituto de Química.

‡ Instituto de Física, Universidade Federal de Bahia, Campus de Ondina, Salvador-BA, CEP: 40210-340, Brazil.

10.1021/jp0274482 CCC: $25.00
Published on Web 07/23/2003

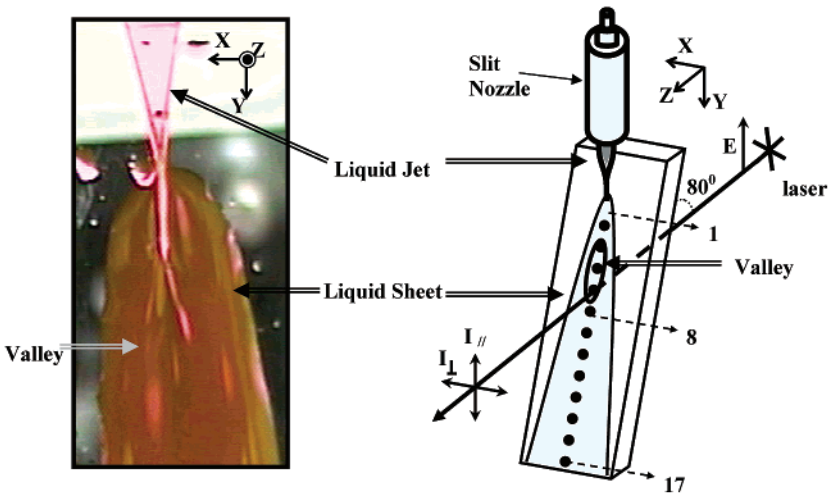

Figure 1. Liquid thin film flowing on a solid surface. Left: photo of the liquid film; right: scheme of the liquid film showing 1, 8, and 17 downstream positions and the fluorescence components parallel ($I_{||}$) and perpendicular ($I_{\perp}$) to the laser electric field (E).

Steady-state fluorescence depolarization by polarized laser-induced fluorescence technique (PLF) determines the polarization of the emitted fluorescence, without resolving fluorescence in wavelength or intensity. In PLF, a vertically polarized laser beam excites fluorescent probes within the sample. Their absorption is proportional to the cosine square of the angle between the molecular transition dipole moment and the laser beam electric field. The flow of the liquid causes a preferential molecular orientation of the probe within the liquid in the downstream direction[8] that is photoselected by the laser. If the dipole is parallel to a longitudinal molecular axis (as for rhodamine, the probe used in this work), mainly the nearly vertical molecules will absorb laser radiation.

In PLF, the fluorescence emission is differentiated on the basis of its polarization and compared with laser polarization. Fluorescence depolarization data can be interpreted either as a bidimensional phenomenon in terms of polarization (P)[9] or as a three-dimensional phenomenon in terms of anisotropy (r):[10,11]

$$P = \frac{I_{||} - I_{\perp}}{I_{||} + I_{\perp}} \tag{1}$$

$$r = \frac{I_{||} - I_{\perp}}{I_{||} + 2I_{\perp}} \tag{2}$$

During their excited-state lifetime, the photoselected probes may or may not rotate, depending on the mobility of neighboring molecules and their chemical environment. For PLF of flow-induced (FI) systems (PLF−FI), polarization is maximum if the molecules are still in the downstream direction when they fluoresce. For a thin liquid sheet flowing on a solid surface, polarization and anisotropy will be high when interaction at the interface is low, because the liquid molecular domains[12] will be aligned with the flow.[6] Both wetting and surface drag decrease and liquid molecules slip more easily downstream. If the interaction between the solid surface and the flowing liquid is greater, there is increased wetting efficiency. Surface drag propagates through adjacent liquid flow layers decreasing slip. Microturbulence can then develop, generating misaligned molecular domains at the interface and decreasing both the polarization and anisotropy imposed by FI.

Thus far, fluorescence depolarization obtained by PLF−FI has been reported in specific applications without wider concern with the range of validity of the method itself.[5−7] It is essential to extend these studies to a wider range of dynamic solid−liquid interfacial tensions (Γ_{SL}), resulting from changes in chemical constitution, to validate PLF−FI as a sensitive method for changes in intermolecular forces at flowing liquid−solid interfaces. It is also necessary to identify the relevant experimental variables and their interdependence.

The aim of this paper is to assess PLF−FI efficiency for the evaluation of the dynamic Γ_{SL} of liquid thin films flowing without boundaries on solid substrates. To attain this, we acquired bidimensional polarization maps of 10 interfaces with different chemical constitutions (varying either the solid substrate or the liquid). Interfaces had different Γ_{SL}, as monitored by contact angle measurements. Also, principal component analysis (PCA),[13,14] a multivariate statistical treatment of data, and hierarchic cluster analysis (HCA) were applied to the PLF−FI polarization data for each interface. Although there are in the literature several reported applications of PCA to fluorescence data,[15,16] this is the first time it has been applied to fluorescence depolarization data and to evaluate dynamic Γ_{SL} for thin liquid films flowing on solid surfaces.

2. Materials and Methods

The apparatus employed to study PLF−FI of thin liquid films flowing on solid surfaces (Figure 1) was developed recently by Quintella et al.[7] The experiment consists of pumping a liquid at a high flow rate, through a thin slit nozzle; the liquid impinges on a solid surface at 10 degrees with respect to the vertical, generating a thin liquid film flowing without boundaries on the solid surface (Figure 1). Fluorescence was induced by focusing the laser on a small spot. Polarized laser-induced fluorescence was bidimensionally mapped by varying the vertical and horizontal position of the sample relative to the laser spot.

Two polished sapphire slit nozzles were used to produce liquid films with initial thicknesses of 100 μm or 300μm.

The liquid film can have three possible velocity profiles[8,9,17] at the moment it impinges on the solid surface: one Gaussian parallel to the surface (profile 1), two Gaussians parallel superposed by two Gaussians perpendicular to the surface (profile 2), and a Gaussian perpendicular to the surface (profile 3).

Four flow velocities were used: 143, 204, 220, and 246 cm s^{-1}.

While flowing on the solid surface the liquid film first increases its width, generating a middle valley (Figure 1). When

TABLE 1: Contact Angles (θ_c) and Their Cosines, Obtained for Monoethylene Glycol (MEG) on Solid Surfaces

map	solid[a]	solute[b]	[solute] (mol L^{-1})	$\theta_c \pm 2°$	$\cos\theta_c \pm 0.01$
M1	SnO_2	none	none	44°	0.72
M2, M3, M4	Bsi	none	none	32°	0.85
M5	PVA	none	none	28°	0.88
M6	LAS	none	none	15°	0.96
M7	Bsi	SDS	3.5×10^{-4}	18°	0.95
M8	Bsi	SDS	4.0×10^{-3}	22°	0.93
M9	Bsi	PEO	3.5×10^{-7}	15°	0.96
M10	Bsi	PEO	saturated	24°	0.91

[a] Solid surfaces: tin dioxide (SnO_2), borosilicate (Bsi), poly(vinyl alcohol) (PVA), and linear alkylbenzene sulfonate (LAS). [b] Dissolved surfactants: sodium dodecyl sulfate (SDS) and poly(ethylene oxide) (PEO).

the width is maximum, two lateral converging streams are formed. The flow thickness ranged from 50 μm at the valley to 1000 μm at the borders. Depending on adhesion, this pattern can have different formation times,[6] thus occurring at different downstream positions.

The liquid employed was monoethylene glycol from Merck (MEG) (catalog number 10921, 99.5% purity). A constant-temperature bath[18] kept the liquid flow at (15.0 ± 0.5) °C.

Rhodamine 6G (Lambdaphysik, 99.99% purity) was used as the fluorescent probe at a concentration[6] of 1.9×10^{-3} mol L^{-1}. This concentration was chosen to avoid quenching due to Förster transfer[19] or dimer formation. MEG has a viscosity higher than water or ethanol and dimer formation only occurs above about 10^{-2} mol L^{-1} at the temperature used.[19]

Adhesion or Γ_{SL} at the interface of flowing liquid−solid substrates was varied in two ways: by adding surfactants to the liquid flow and by changing the chemical constitution of the solid surface. Parameters for each liquid−solid surface are shown in Table 1.

Four surfactant solutions were used: two of the detergent sodium dodecyl sulfate (SDS) (Sigma L-6026, 99% purity) at 3.5×10^{-4} and 4.0×10^{-3} mol L^{-1} and two of the long chain polymer poly(ethylene oxide) (PEO) (ca. 4 000 000, Aldrich 18,946-4) at 3.5×10^{-7} mol L^{-1} and as a saturated solution. All SDS concentrations were submicellar, as determined by conductivity and surface tension.

Chemical constitution of the solid surfaces was chosen to provide a range of Γ_{SL}, these being tin dioxide, PVA, LAS, and borosilicate.

All solid surfaces had the dimensions of a microscope slide (75 mm × 25 mm × 0.8 mm), were structureless, and had roughness below 10 nm, as determined by AFM. Borosilicate was maintained for 10 min in an ultrasonic bath with ethanol and dried for 15 min in an oven at 50 °C. The tin dioxide (SnO_2) substrate[20] consisted of a 200 nm layer of SnO_2 on borosilicate. A 400 nm layer of poly(vinyl alcohol) (PVA) from Carlo Erba was deposited on the SnO_2 surface by mixing a 5% aqueous solution with a Headway P101 shaker at 2500 rpm for 30 s. The polymer layer was horizontally baked in an oven at 80 °C for 60 min. Substrate with linear alkylbenzene sulfonate (LAS) was prepared by evaporating a commercial detergent of low purity, followed by deposition on borosilicate by consecutive immersion in a saturated solution and baking in an oven at 80 °C for 60 min. Absorption spectra of the substrates, obtained before and after the experiment, showed no adsorbed rhodamine.

The experimental setup employed to acquire the fluorescence depolarization maps by PLF−FI has been described in detail elsewhere.[7] It consisted of a PLF optical line (Figure 2) in which fluorescence is induced by a vertically polarized laser. Laser

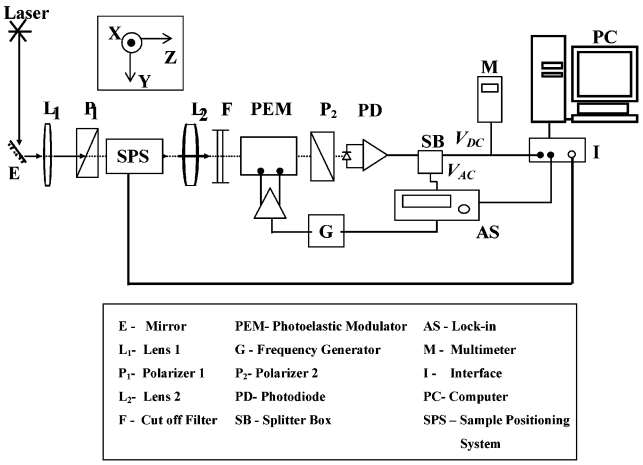

Figure 2. Experimental setup for polarized laser-induced fluorescence (PLF) to detect fluorescence depolarization.

power was kept below transition saturation and ranged from 30 to 250 mW. Fluorescence detection was made in function of its vertical and horizontal polarization components.

3. Results and Discussion

Since solid surface roughness was lower than 10 nm for all surfaces and polarization maps were acquired with resolution of ca. 0.25 mm, the experiment is not able to detect any surface structures present. Thus, the results of dynamic wetting can be interpreted as depending mainly on interfacial interactions due to chemical composition.

Contact angles (θ_c) were acquired for each substrate (Table 1) to evaluate their Γ_{SL}, that is, adhesion, which is directly proportional to the cosine of θ_c.[1] Increasing values of $\cos\theta_c$ imply that wetting efficiency and adhesion increase as well; thus, drag at the interface will also increase. For interfaces without solutes, Γ_{SL} increased in the order SnO_2, Bsi, PVA, and LAS. When surfactant was present in solution, $\cos\theta_c$ increased substantially. An increase in surfactant concentration decreased the interfacial tension. For the surfactant LAS as substrate, $\cos\theta_c$ was quite small. This was attributed to dissolution of LAS in MEG during image acquisition as the drops spread on the LAS surface.

Polarization was obtained in percentage and normalized according to eq 1. The normalization with respect to the total fluorescence (LIF) makes the data independent of fluorescence intensity (within the range used here) and emphasizes the changes due to fluorescence depolarization. A correction factor due to birefringence of the optical components was applied.[7]

Maps of the polarization and anisotropy of the thin flowing liquid films were acquired for 17 mm downstream and 6 mm across stream, yielding maps of 17 × 17 points with 0.1 mm^2 spatial resolution and repeatability better than 0.1%.

Owing to the similarity of the patterns in the polarization and anisotropy maps, only polarization maps are discussed in this study. Two of the 10 maps are shown in Figure 3.

The average polarization (P_{av}) for each map was obtained by averaging the polarization values obtained at each point of the map. The P_{av} of the dye in a static (nonflowing) condition was 7.2%, being lower than the P_{av} obtained under dynamic (flowing) conditions.

Table 2 shows the dependence of P_{av} on experimental hydrodynamic variables for the MEG/Bsi interface. Fixing the flow rate (maps M2 and M3), P_{av} decreased for impinging velocity profile number 2 because of generation of inner streams

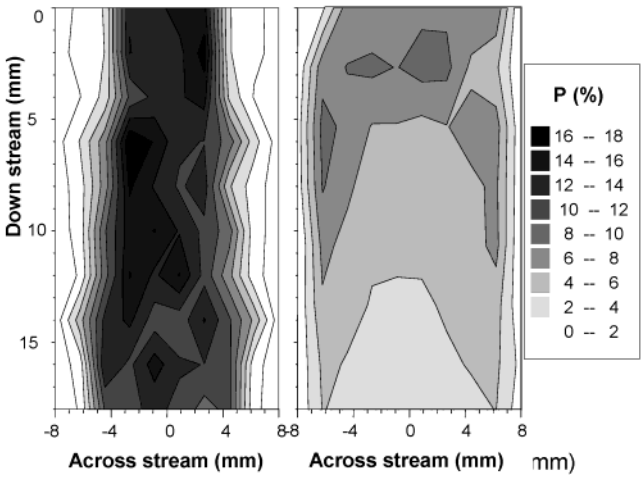

Figure 3. Fluorescence depolarization shown as polarization for two maps from Tables 2 and 3. Left: map obtained with monoethylene glycol (MEG) flowing on borosilicate (M3). Right: map obtained with solution of sodium dodecyl sulfate in monoethylene glycol (MEG), at 4.0×10^{-3} mol L^{-1}, flowing on borosilicate (M8).

TABLE 2: Effect of Hydrodynamic Experimental Variables on the Average Polarization (P_{av}) of Maps for Thin Films of Monoethylene Glycol (MEG) Flowing without Boundaries on Borosilicate (Bsi)[a]

map	VP	V (cm s^{-1})	P_{av} (%)
M2	2	246	8.8
M3	1	246	10.2
M4	1	143	10.5

[a] Variables: flow rate of liquid flow (V) and impinging velocity profile (VP).

within the flowing liquid film. For the same impinging velocity profile (maps M3 and M4), a decrease in the flow rate increased P_{av}. This is because a flow rate increase causes the valley (Figure 1), where polarization is higher, to occur further downstream, at the bottom of the region mapped. Thus, for high flow rates, the vertical movement of the liquid film also depends on the stress imposed by the liquid circulation system as well as gravity and surface drag. Horizontal movements were still mainly dependent on drag at the interface because of adhesion.

No contribution to P_{av} was observed from initial film thickness within the range used, which may be explained by changes in the original thickness as a function of the wetting efficiency as the liquid flows on the solid substrate.

Thus, in addition to its dependence on the static interfacial tension Γ_{SL} (evaluated by θ_c), P_{av} is affected by impinging velocity profile 2. As the flow rate increased over 220 cm s^{-1}, the polarization decreased which may be attributed to a saturation of polarization because of turbulence setting in. Thus, profile 2 was not used and the flow rate was kept below 220 cm s^{-1}.

Table 3 presents the effect of Γ_{SL} on P_{av} for the 10 interfaces studied. Upon changing the chemical constitution of the solid substrate (Table 3, maps M1, M4, and M6) P_{av} increased as Γ_{SL} and wetting efficiency decreased. Interfacial drag became weaker and molecular domains flow downstream more freely, staying better aligned with the flow and increasing P_{av}.

For PVA (Table 3, map M5), the opposite occurs. P_{av} is higher than that of Bsi, although the latter had a lower Γ_{SL}. This effect was previously seen by Quintella et al.[5] and was attributed to the fact that the PVA surface had been rubbed in the flow direction, which increased the orientation of the surface groups along the downstream direction, favoring wetting in the downstream direction and inducing a downstream alignment and, consequently, increasing polarization.

TABLE 3: Effect of Solid−Liquid Interfacial Tension on the Average Polarization (P_{av}) of Maps for Thin Films of Monoethylene Glycol (MEG) Flowing without Boundaries[a]

map	solid[b]	solute[b]	[solute] (mol L^{-1})	P_{av} (%)
M1	SnO_2	none	none	11.4
M4	Bsi	none	none	10.5
M5	PVA	none	none	12.1
M6	LAS	none	none	13.5
M7	Bsi	SDS	3.5×10^{-4}	4.3
M8	Bsi	SDS	4.0×10^{-3}	4.4
M9	Bsi	PEO	3.5×10^{-7}	5.4
M10	Bsi	PEO	saturated	3.8

[a] Γ_{SL} was varied either by changing chemical constitution of solid substrates or by surfactant addition to MEG. [b] Abbreviations: borosilicate (Bsi), tin dioxide (SnO_2), poly(vinyl alcohol) (PVA), linear alkylbenzene sulfonate (LAS), detergent sodium dodecyl sulfate (SDS), and long-chain polymer (ca. 4 000 000) poly(ethylene oxide) (PEO).

When the flowing liquid sheet contained dissolved detergent, P_{av} strongly decreased (Table 3, maps M7, M8, M9, and M10) while with detergent as substrate (Table 3, map M6 for LAS) it reached its highest value. This may be explained by anchoring of the polar groups of LAS detergent molecules on the borosilicate surface, aligning the alkyl groups with the flow that might form a layer over which ethylene glycol flows almost without interacting with borosilicate, resulting in high slip. As a result, MEG molecular domains increasingly align with the flow in the downstream direction, increasing P_{av}. SDS (Table 3, maps M7 and M8) was dissolved directly in the liquid phase. Its concentration at the interface was low and it is likely that at the interface its distribution was not homogeneous (unlike the deposited surfactant) causing hindrance to ethylene glycol flow and misalignment of molecular domains and reducing P_{av}.

For the long chain polymer PEO (Table 3, maps M9 and M10), interaction with the Bsi surface could take place at multiple points of the polymer chain, which could induce turbulence, misaligning molecular domains and reducing P_{av}. In addition, it is known that PEO forms molecular clusters in the bulk when no intermediate solvent is used and the temperature is low.[21] If this is happening, the polarization would be reduced. The increase of the contact angle with increasing PEO concentration (Table 1) shows a decrease in the strength of the interaction with the surface. This is compatible with an increase in the aggregation level as the solution becomes more concentrated. Further studies of PEO dissolved in MEG are needed to confirm this hypothesis.

Compared to SDS (Table 3, maps M7 and M8), an increase in PEO concentration (Table 3, maps M9 and M10) resulted in a pronounced decrease of P_{av}. This might also be consistent with intensification of the aggregation in the bulk.[21]

Multivariate Statistical Data Treatment. To interpret the maps obtained at a level beyond their average polarization (P_{av}), the multivariate statistical method of principal component analysis (PCA) [13,14] was applied. This approach was chosen because it is able to interpret essential information not only from the variables themselves but also from the way they vary in relation to one another, that is, how they co-vary, providing important chemical information.[22] Hierarchic cluster analysis (HCA) [23] gave the degree of similarity among the polarization maps of the various interfaces.

To prepare PCA data entries, the average of the polarization values acquired at the same downstream position (P_{down}) was calculated for each map and a column of data built with these

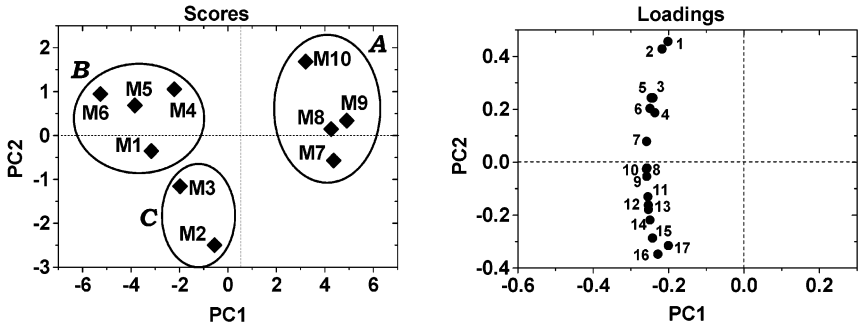

Figure 4. Graphs of PC2 versus PC1. Left: scores for polarization maps. Right: loadings (each number stands for the *i*th position downstream).

TABLE 4: Polarization Average for Each downstream Position (P_{down}) Used as the Data Entry Matrix for Principal Component Analysis (PCA) and Hierarchic Cluster Analysis (HCA)[a]

downstream position	M1	M2	M3	M4	M5	M6	M7	M8	M9	M10
1	9.5	4.4	4.0	11.6	12.7	16.1	3.7	4.6	3.8	7.3
2	9.5	4.5	6.1	10.3	12.0	15.0	3.2	4.5	4.4	7.3
3	9.5	6.2	10.8	10.3	12.0	15.0	3.2	4.5	4.4	7.3
4	11.0	8.1	9.7	11.0	12.0	11.0	3.5	4.4	4.2	9.0
5	10.5	5.9	9.7	12.0	11.9	13.4	4.2	4.2	3.8	6.4
6	12.1	6.3	10.2	12.0	13.0	13.4	4.4	4.6	3.8	6.4
7	12.1	8.6	10.1	12.0	13.0	14.7	4.4	4.6	3.7	5.5
8	12.8	9.0	12.4	12.0	13.0	13.6	4.4	4.5	3.6	5.1
9	12.9	9.3	12.1	11.0	12.6	13.6	4.3	4.6	3.6	5.1
10	12.9	9.0	11.2	11.0	12.6	14.1	4.3	4.6	3.6	4.6
11	13.0	10.4	12.9	11.0	13.0	13.4	4.0	4.2	3.6	4.4
12	13.0	11.5	11.4	10.0	13.0	13.4	3.7	3.8	3.6	4.4
13	12.0	11.3	11.6	9.6	12.3	13.9	3.6	3.6	3.5	4.1
14	12.0	10.7	12.4	9.0	11.7	12.7	4.0	3.5	3.5	4.0
15	11.3	11.9	11.0	9.0	10.6	12.6	4.7	4.0	3.7	3.7
16	9.3	11.5	11.7	8.4	10.0	12.3	5.8	4.9	3.6	3.5
17	10.3	11.5	6.1	8.0	9.7	10.9	7.0	5.5	3.6	3.4

[a] Columns and rows correspond, respectively, to maps and downstream positions (see Figure 1).

averages. Columns related to each map were juxtaposed, producing a data matrix (Table 4). In this matrix, columns correspond to the P_{down} values for each map and rows to the *i*th position downstream in each of the 10 maps. This matrix was transposed and autoscaled prior to PCA data treatment.

The PCA first principal component (PC1) was responsible for 86.8% of the variance and the second (PC2) for 8.8%. PC1 and PC2 together were responsible for 95.6% of the variation in P_{down} for each map.

Figure 4 presents graphs of PC1 × PC2 scores (left) and loadings (right). PC1 × PC2 scores (Figure 4, left) fell into three different groups: solute addition to MEG (*A*), change of substrate (*B*), and maps acquired at the highest flow rate (*C*).

PC1 scores ordered the maps in decreasing order of P_{av} (Table 3). In PC1 × PC2 loadings (Figure 4, right), each point stands for a downstream position of the flowing liquid film. For PC1 loadings, all positions along the liquid film had nearly the same value (-0.23 ± 0.3) since intermolecular interactions established at the interface should be relatively constant for a constant chemical constitution.

Positive PC1 scores (Figure 4, left) corresponded to maps in which the flowing liquid film contained dissolved surfactants and presented low P_{av} (maps M7, M8, M9, and M10 in group *A*).

The map obtained for the detergent substrate (map M6 for LAS) was on the left in group *B* at negative PC1 scores.

As seen before, an increase in the concentration of PEO (Table 3, maps M9 and M10) compared to SDS (Table 3, maps M7 and M8), resulted in a pronounced increase of P_{av} and, consequently, these were further apart in PC1 × PC2 scores.

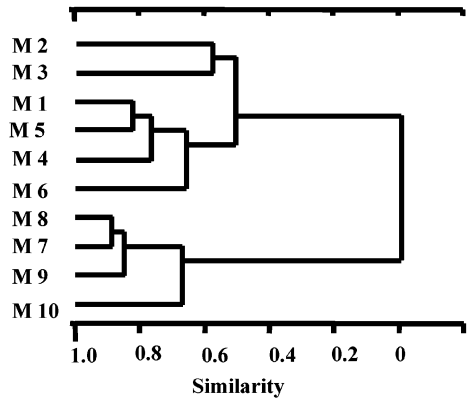

Figure 5. Hierarchic cluster analysis dendogram (HCA) of polarization maps.

PC2 positive and negative loadings (Figure 4, right) correspond, respectively, to the first and second halves of the flow. They show the downstream position contribution to P_{down} in each map. In group *B* (left Figure 4), solid surfaces with higher Γ_{SL} for ethylene glycol had maximum polarization at the top of the flowing liquid film (borosilicate-M4, PVA-M5, and LAS-M6). As Γ_{SL} decreased, maximum polarization moved further downstream (SnO_2 −M1). Similarly, group *A* has higher contributions to P_{av} from the top half of the flow because of reduced interaction with the solid substrate; drag was weak and it preserved memory of the flow alignment downstream.

Group *C* (left Figure 4) contained maps for liquid films at the highest flow rate (maps M2 and M3) where, unlike in the other maps, valleys occur in the second half of the flow.

Figure 5 presents the dendogram from HCA, which divides the maps into three groups. Their similarity increased with weaker adhesion or lower Γ_{SL}.

The bottom branch includes the maps from group *A* (left Figure 4) with dissolved surfactants, which have lower P_{av} (Figure 5, maps M7, M8, M9, and M10). Similarity was higher among the maps for SDS and decreased as the PEO concentration increased.

The central branch corresponds to group *B* (left Figure 4) and consisted of maps for solid substrates of different chemical constitutions (Figure 5, maps M1, M4, M5, and M6).

The top branch includes the maps of group *C* (left Figure 4) for liquid films at the highest flow rate (Figure 5, maps M2 and M3), showing the dependence of PLF−FI on this variable.

4. Conclusion

Fluorescence depolarization of liquid films flowing without boundaries on solid surfaces, obtained by PLF−FI, proved to

be efficient for relative dynamic Γ_{SL} evaluation. It is sensitive to changes in the chemical constitution of both the solid substrate and the flowing liquid. It distinguished between deposited and dissolved surfactants and was sensitive to the surfactant concentration. This reflects the sensitivity of PLF−FI to adhesion. Differences in adhesion result in different wetting efficiencies and control interfacial drag, which is propagated into the flow through MEG intermolecular hydrogen bonding.

Among the experimental hydrodynamic variables, only impinging velocity profile 2 and flow rates over 220 cm s^{-1} affected the average polarization (P_{av}).

Dissolved surfactant decreased P_{av}, while a solid surfactant substrate increased P_{av} because of a decrease in interfacial dynamic adhesion. The latter observation is strong evidence that static Γ_{SL} might be different from dynamic Γ_{SL} in these flows.

Statistical data treatment of maps was performed by principal component analysis (PCA) and hierarchic cluster analysis (HCA). The averaged polarization for each downstream position (P_{down}) gave results similar to the average polarization for each map (P_{av}). PCA divided the systems into three groups: surfactant addition to MEG, different chemical constitution of the substrate, and highest flow rate. Downstream position was not a determining factor, which confirms that PLF−FI is influenced by chemical composition and not physical effects of flow hydrodynamics. The HCA dendogram showed higher similarity for smaller Γ_{SL} because of weaker adhesion and wetting efficiency, causing drag propagation from the interface to decrease.

Acknowledgment. Grants from Conselho Nacional de Desenvolvimento Científico e Tecnológico (CNPq, Brazil) and PADCT3 partially supported this work. We acknowledge CenPRA/ITI (Profa. P. Mammana) for providing the SnO_2 and PVA surfaces, IF/USP (A. M. P. Passaro) for the atomic force microscopy, and A. J. McCaffery for the sapphire slit nozzles. A.M.V.L. and A.P.S.M. acknowledge undergraduate research fellowships from PIBIC-CNPq, C.C.G. acknowledges a DPhil scholarship from CAPES, and C.M.Q. acknowledges a senior research scholarship from CNPq.

References and Notes

(1) Adamson, A. W.; Gast, A. P. *Physical Chemistry of Surfaces*; John Wiley & Sons: New York, 1997.
(2) Lam, C. N. C.; Wu, R.; Li, D.; Hair, M. L.; Neumann, A. W. *Adv. Colloid Interface Sci.* **2002**, *96*, 169−191.
(3) Extrand, C. W. J. *Colloid Interface Sci.* **2002**, *248*, 136−142.
(4) Blake, T. D.; De Coninck, J. *Adv. Colloid Interface Sci.* **2002**, *96*, 21−36.
(5) Quintella, C. M.; Lima, Â. M. V.; Gonçalves, C. C.; Watanabe, Y. N.; Schreiner, M. A.; Mammana, A. P.; Pepe, I.; Pizzo, A. M. *J. Colloid. Interface Sci.* **2003**, *262* (1), 221−226.
(6) Quintella, C. M.; Gonçalves, C. C.; Pepe, I.; Lima, A. M. V.; Musse, A. P. S. *J. Braz. Chem. Soc.* **2001**, *12*, 780−786 (available on line, in English, at http:/ /jbcs.sbq.org.br/jbcs/2001/vol12_n6/14.pdf).
(7) Quintella, C. M.; Gonçalves, C. C.; Pepe, I.; Lima, A. M. V.; Musse, A. P. S. *J. Autom. Methods Manage. Chem.* **2002**, *24*, 31−39 (available on line in English at http://taylorandfrancis.metapress.com).
(8) Kenyon, A. J.; McCaffery, A. J.; Quintella, C. M. *Mol. Phys.* **1991**, *72*, 965.
(9) Kenyon, A. J.; McCaffery, A. J.; Quintella, C. M.; Winkel, J. F. *Mol. Phys.* **1991**, *74* , 871.
(10) Kawski, A. *Crit. Rev. Anal. Chem.* **1993**, *23*, 459.
(11) Lakowicz, J. R. *Principles of Fluorescence Spectroscopy*; Plenum Press: New York, 1983.
(12) Juzeliunas, G. J. *J. Lumin.* **1990**, *46*, 201.
(13) Martens, H.; Naes, T. *Multivariate Calibration*; John Wiley & Sons: New York, 1989.
(14) Geladi, P.; Kowalski, B. R. *Anal. Chim. Acta* **1986**, *185*, 1−17.
(15) Bro., R. *Chemom. Intell. Lab. Syst.* **1999**, *46*, 133−147.
(16) Amador-Hernandez, J.; Fernandez-Romero, J. M.; Castro, de M. D. L. *Anal. Chim. Acta* **2001**, *488*, 61−69.
(17) Quintella, C. M.; Gonçalves, C. C.; Musse, A. P. S.; McCaffery, A. J. *Exp. Fluids* **2003**, in press.
(18) Quintella, C. M.; Gonçalves, C. C.; Lima, A. M. V.; Guimarães, A. K.; dos Santos, J. C.; Pepe, I. *Quim. Nova* **2003**, *26*, 130−132.
(19) Bojarski, P.; Jankowicz, A. *J. Lumin.* **1999**, *81*, 21−31.
(20) Baranauskas, V.; Jingguo, Z.; Mammana, A. P.; Santos, T. E. A.; Schreiner, M. A.; Mammana, C. I. Z. *Sens. Actuators, A* **2002**, *85* (1−2), 90−94.
(21) Duval, M.; Sarazin, D. *Polymer* **2000**, *41*, 2711−2716.
(22) Wold, S.; Sjöström, M. *Chemom. Intell. Lab. Syst.* **1998**, *44*, 3−14.
(23) Matthias, O. *Chemometrics: statistics and computational in analytical chemistry*; Wiley-VCH Verlag GmbH: Weinheim, FRG, 1999.